RIDGELET-BASED TEXTURE CLASSIFICATION OF TISSUES IN COMPUTED TOMOGRAPHY

Lindsay Semler[a], Lucia Dettori[a], and Brandon Kerr[b]
[a] DePaul University 1E. Jackson, Chicago, IL 60604
[b] Trinity University One Trinity Place San Antonio, TX 78212
lsemler@cti.depaul.edu, William.Kerr@Trinity.edu, ldettori@cti.depaul.edu

ABSTRACT
The research presented in this article is aimed at the development of an automated imaging system for classification of tissues in medical images obtained from Computed Tomography (CT) scans. The article focuses on using ridgelet-based multi-resolution texture analysis. The approach consists of two steps: automatic extraction of the most discriminative texture features of regions of interest and creation of a classifier that automatically identifies the various tissues. The classification step is implemented through a decision tree classifier based on the cross-validation Classification and Regression Tree approach. The discriminating power of several ridgelet-based texture descriptors are investigated. Preliminary results indicate that Entropy signatures are the most effective descriptors for ridgelets. Generally, multiple resolutions have a higher discriminating power than a single resolution level, and in this application, combining two resolutions instead of three increases performance.

KEY WORDS
Texture Classification, Multi-resolution Analysis, Ridgelet, Computed Tomography

1. Introduction

The research presented in this article is part of an ongoing project [1] – [3] aimed at developing an automated imaging system for classification of tissues in medical images obtained by Computed Tomography (CT) scans. Classification of human organs in CT scans using shape or gray level information is particularly challenging due to the changing shape of organs in a stack of slices in 3D medical images and the gray level intensity overlap in soft tissues. However, healthy organs are expected to have a consistent texture within tissues across multiple slices. This research focuses on using ridgelet-based multi-resolution texture analysis for the classification of tissues from normal chest and abdomen CT scans. The approach consists of two steps: automatic extraction of the most discriminative texture features of regions of interest and creation of a classifier that automatically identifies the various tissues. Several ridgelet-based texture descriptors are investigated, and an in depth study of the discriminating power of multiple resolution levels is carried out. The classification step is implemented through a decision tree classifier based on the cross-validation Classification and Regression Tree (C&RT) approach [1]. This paper offers a comprehensive analysis determining the optimal texture descriptors and resolution depth for the ridgelet transform as applied to CT scans. It also includes a comparison of these ridgelet-based features with previous results of wavelet-based features.

Texture is a commonly used feature in the analysis and interpretation of images. Texture can be characterized by a set of local statistical properties of the pixel grey level intensity, measuring variations in a surface such as smoothness, coarseness and regularity. Common tools in extracting texture for classification include: run-length statistics [9], co-occurrence matrices [8], statistical moments, and multi-resolution techniques such as the wavelet transform [2].

Multi-resolution analysis has been successfully used in image processing and number of applications to texture classification has been proposed over the past few years [7]. Several studies have investigated the discriminating power of wavelet-based texture features applied to various fields. More recently, applications of the ridgelet transform to image contrast enhancement and image denoising have been explored [3]. To the author's knowledge, ridgelet-based texture classification has been applied only in the context of natural images [4]. This research focuses on the texture classification using features derived from the ridgelet transform of the images.

1.1 Multi-resolution Analysis

Multi-resolution analysis allows for the preservation of an image according to certain levels of resolution or blurring. Essentially, multi-resolution analysis allows for the zooming in and out of the underlying texture structure within the image. Therefore, the texture extraction is not effected by the size of the pixel neighborhood. This multi-resolution quality is why wavelets have been useful in image compression, image de-noising, and image classification. Wavelets have been an area of research in many texture classification applications [7] and have been useful in capturing texture information and edge detection in natural images, such as detecting the vertical outline of a skyscraper. Evolving from the wavelet transform, the

finite ridgelet transform has developed within the past few years.

Understanding the properties of the wavelet transform is essential to the comprehension of the strengths of the ridgelet transform. The wavelet transform extracts directional details that capture horizontal, vertical and diagonal activity. However, these three linear directions are limiting, and might not be able to capture enough directional information in noisy images, such as medical CT scans. Ridgelets, like wavelets, provide multi-resolution texture information, however they capture structural information of an image based on multiple radial directions in the frequency domain. The multi-directional capabilities of the ridgelet transform proves to be very effective in the texture classification of the more organic textures in medical images.

Once the ridgelet transform is applied, several statistical measures are calculated in order to capture the texture information. These statistical measures provide texture descriptors that are used in the classifier to create classification rules. Typical statistical measures used in texture classification in image processing are: mean, standard deviation, energy, entropy, contrast, homogeneity, variance, correlation, maximum probability, sum-mean, cluster tendency, inverse difference moment. Because these statistics are being applied to the ridgelet transform, which extracts contrast of pixel pairs in radial directions, not all of these statistical measures would be appropriate to use. Other research in multi-resolution texture analysis as seen in [4] and [6], use statistics such as energy, mean, and standard deviation. This paper investigates the use of several combinations of four descriptors: energy, entropy, mean and standard deviation. Preliminary results indicate that Entropy signatures are the most effective descriptors for ridgelets. These ridgelet-based descriptors out-performed Haar, Daubechies, and Coiflet wavelet-based descriptors on the same data set.

1.2 The Ridgelet Transform

The continuous ridgelet transform may be constructed as a wavelet transform in the Radon domain. Candes and Donoho developed the ridgelet transform as discussed in [5], to overcome the disadvantage of the directional limitations of the 2D wavelet transform. The continuous ridgelet transform can be defined from a 1-D wavelet function oriented at constant lines and radial directions The continuous ridgelet transform (CRT) in R^2 is defined by:

$$CRT_f(a,b,\theta) = \int_{R^2} \psi_{a,b,\theta}(x) f(x) dx$$

where the ridgelet $\Psi_{a,b,\theta}(x)$ in 2-D are defined using a wavelet function :

$$\psi_{a,b,\theta}(x) = a^{-\frac{1}{2}} \psi((x_1 \cos\theta + x_2 \sin\theta - b)/a)$$

This is oriented at angles θ, and is constant along the lines. $x_1 \cos\theta + x_2 \sin\theta = const$ for details see, [5].

Essentially, the ridgelet radial lines are defined by a slope θ, and an intercept b. The continuous ridgelet transform is similar to the continuous wavelet transform except that point parameters *(x,y)* are now replaced by line parameters *(b, θ)*. Generally speaking, wavelets represent objects with point singularities, while ridgelets are able to represent objects with line singularities.

One of the challenges of using ridgelets for texture classification of images is the discretization of the ridgelet transform. Since the radon transform is polar, we cannot implement direct digital forms of the continuous formula. Thus, the finite ridgelet transform was applied using the technique described in [3]. In the article, the discrete ridgelet transform is obtained by applying a 1-dimensional wavelet transform to slices of the radon transform of the image. The radon transform provides direction information in the frequency domain. This transform is applied by partially reconstructing the most significant coefficients along radial directions in the Fourier transform.

2. Methodology

The standard texture classification algorithm includes three main steps: the segmentation of regions of interest, the extraction of texture features, and the creation of a classifier [see figure 1].

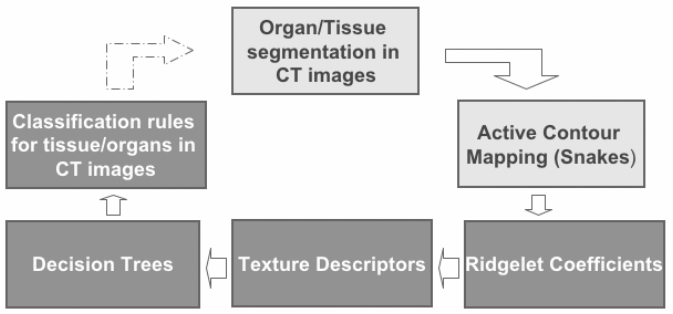

Figure 1: Methodology Diagram

2.1 Data Set

Our preliminary results were obtained on 3D data extracted from two normal chest and abdomen CT studies from Northwestern Memorial Hospital. The data consisted of 340 2D DICOM consecutives slices, each slice being 512 x 512 and having 12-bit gray level resolution. Ideally, a radiologist should segment the training set in order to have ground truth images to train the classifier. However, since this was not available, the organs were segmented using a supervised Active Contour Models ("Snake") algorithm. Five tissues were segmented from the initial data: heart, liver, spleen, kidney, and backbone. An Active Contour Model is a function that recreates the boundary of a particular object when given a set of initial points around the region of interest, as well as values for parameters that determine

the boundary's smoothness [1]. The segmentation process generated the following slices: 140 Backbone, 52 Heart, 58 Liver, 54 Kidney, and 40 Spleen. Since wavelets and ridgelets are extremely sensitive to contrast in the gray level intensity, the segmented images need further processing. In order to effectively use ridgelet-based texture descriptors, it was necessary to eliminate all background pixels to avoid mistaking the edge between the artificial background and the tissue as a texture feature. Each slice was therefore further cropped, and only square 31 x 31 sub-images fully contained in the interior of the segmented area were generated. Images of size 31 x 31 were chosen since the digital ridgelet requires a prime-size square image; this is discussed in more detail in [3]. Figure 2 shows an example CT scan and a segmented and cropped slice of heart.

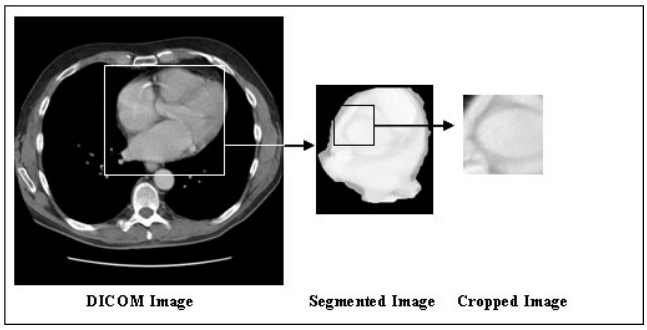

Figure 2: Sample Segmentation

The cropping of the images resulted in 2,091 slices of "pure" single-organ tissue (363 Backbone, 446 Heart, 506 Liver, 411 Kidney, 364 Spleen). This data set was split into a training set and a testing set for the cross-validation decision trees described in Section 2.3.

2.2 Feature Extraction

The Finite Ridgelet Transform, as presented in [3], was implemented in two main steps: application of a radon transform and an application a 1-dimensional wavelet transform. The radon transform was computed by first calculating the 2-dimensional fast Fourier transform of the image, and then applying a 1-dimensional inverse Fourier transform on 32 radial directions of the radon projection. The radial directions were found using digital approximations, due to the digital limitations. This approach captured exact samples from the image, however used approximate radial angles. Since the images were of size 31 x 31, 32 radial directions were extracted by using digital approximations, further described in [3]. A one-dimensional wavelet was applied to each of the 32 radial directions.

The Haar wavelet was chosen for its superior discriminating power in the same data set as researched in [2]. The Haar wavelet is the oldest and simplest orthonormal wavelet. It is conceptually simple and exactly reversible without edge effects, which are characteristic of other wavelets. The Haar transform does not have overlapping windows, which reflects only changes between adjacent pixel pairs. These characteristics make them ideal for the application in the finite ridgelet transform. The Haar wavelet was then applied to the radon transform for three levels of resolution. For each of the three levels of resolution and for each of the 32 radial directions, several texture descriptors were then calculated.

In order to extract texture information from the ridgelet representation of the images, several statistics were calculated. The most common statistics calculated on wavelets are mean and standard deviation. The limited literature on ridgelet-based descriptors also suggests the use of a combination of mean, standard deviation, and energy signals (see for example [4]). One of the goals of our research was to identify the most effective texture descriptors for medical images. Mean, standard deviation, energy, and entropy were investigated and their discriminatory power compared. Each of these first order statistics was calculated for each radial direction and resolution level of the wavelet details. The following four feature vectors were investigated: Energy and Entropy signatures averaged over radial directions (EE), Energy, Entropy, Mean, and Standard Deviation signatures averaged over radial directions (EEMS), Energy signatures (Eng), and Entropy signatures (Ent), neither averaged over radial directions. Each of these feature vectors was computed for three levels of resolution yielding: 6 descriptors, 12 descriptors, and 96 descriptors respectively. Our tests indicate that the best results are obtained using the Entropy signatures alone (Ent). The tests also show that Ent ridgelet-based descriptors outperform wavelet-based descriptors (see [2] for details on the wavelet-based algorithm).

2.3 Classification

The classification step was carried out using a decision tree classifier based on the Classification and Regression Tree (C&RT) approach. A decision tree predicts the class of an object from values of predictor variables or texture descriptors. The most relevant texture descriptors are found for each specific organ, and based on those selected descriptors, a set of decision rules are generated. These set of rules are then used for the classification of the each region. Using the C&RT cross-validation approach, each tree's parameter was optimized, including depth of tree, number of parent nodes, and number of child nodes. To evaluate the performance of each classifier; specificity, sensitivity, precision, accuracy rates were calculated from each of the misclassification matrices [see Table 1].

Measure	Definition
Sensitivity	True Positive / Total Positive
Specificity	True Negative / Total Negatives
Precision	True Positive / (True Positive + False Positives)
Accuracy	(True Positives + True Negatives) / Total Sample

Table1: Performance Measures

A misclassification matrix is a table that lists each organ and its true positives, true negatives, false positives and false negatives. The number of true positives is the number of organs that are correctly classified as that organ. The number of true negatives is the number of other organs that are correctly classified as other organs. The number of false positives is the number of organs that are incorrectly classified as that organ. The number of false negatives is the number of organs that are incorrectly classified as other organ.

Specificity measures the accuracy among positive instances, and is calculated by dividing the true negatives by the number of all other organ slices. Sensitivity measures the accuracy among negative instances, and is calculated by dividing the number of true positives by the total number of that specific organ slices. Precision measures the correctness of each organ labeled positive, and is calculated by dividing the number of true positives by the total number of positives. Accuracy reflects the overall correctness of the classifier, and is calculated by adding the true positives and negatives together and dividing by the entire number of organ slices.

In the medical domain, the most important performance measures are both specificity and sensitivity. Optimally one would want both high specificity and high sensitivity measures. However, theoretically these two measures should have a negative correlation; for example as specificity increases, sensitivity should decrease. Since accuracy reflects both the sensitivity and specificity in relation to each other, this descriptor was examined to determine the overall correctness of the classifier.

3. Results

Our results indicate that, for medical images, Entropy signatures are the most effective descriptors for ridgelets. Generally, multiple resolutions have a higher discriminating power than a single resolution level, and combining two resolutions instead of three increases performance in most cases.

Table 2 shows a comparison of the accuracy rates for all feature vectors.

Accuracy	EE	EEMS	Eng	Ent
Backbone	92.6	92.9	94.7	97.3
Heart	78.3	80.0	86.9	93.6
Kidney	83.4	84.9	89.7	92.7
Liver	86.0	86.5	89.7	92.7
Spleen	84.6	84.4	87.6	91.7
Average	85.0	85.7	89.7	93.6

Table 2: Accuracy rate comparison for ridgelet feature

The Entropy signatures (Ent) are in the range 91-97%, and clearly outperformed all other feature vectors. It should be noted that Ent also outperforms wavelet-based texture features, calculated on the same data set whose accuracy rates were in the range 84-93%. Details on the wavelet-based texture classification can be found in [2]. A comparison of all performance measures for Eng and Ent is shown in Table 3. The low performance of EE and EEMS indicate that averaging over directions results in lower discriminating power.

An analysis of the discriminating power of the Entropy feature vector, based on the various resolution levels, was also carried out. The following sets of descriptors were calculated: Ent based on individual levels of resolution (L1, L2, and L3), Ent based on two levels (L12), and Ent based on three levels (L123). The results clearly indicate that individual resolution levels did not have sufficient discriminating power, thus multiple resolutions were needed. Table 4 illustrates the comparison between L12 and L123. On average, L12 performed better than L123. An exception is the heart, for which including the third resolution level improves the results. Mixed results were obtained for liver and spleen. Further investigation for these organs is being carried on.

The results also show that the ridgelet-based texture features outperform wavelet-based descriptors. Table 5 illustrates the comparison of performance rates between ridgelet-based and wavelet-based texture features. Accuracy rates for wavelet-based texture descriptors range between 85 - 93%, while ridgelet-based accuracy rates are in the 91 - 97% range. Overall, the ridgelet-based descriptors have significantly higher performance measures, with accuracy rates approximately 4% higher than any other feature set for all individual organs. This was expected due to the fact that the ridgelet transform is able to capture multi-directional features, as opposed to the wavelet transform which focuses mainly on horizontal, vertical, and diagonal features, which are not dominant in medical CT scan images.

3.1 Future Work

An area of further investigation is the optimization of the radon projection used in the radon transform. Currently, this approach uses digital samples from approximate radial angles. Another possible area of study is the use of interpolation to get approximate digital samples from exact radial angles. Presently, there are several other algorithms for the digital representation of the ridgelet transform; other such algorithms will be explored to investigate their effect on the resulting texture descriptors.

One of the limitations of using ridgelet-based descriptors is the fact that ridgelets are most effective in detecting linear radial structures, which are not the main component of medical images. A recent extension of the ridgelet transform is the curvelet transform. Curvelets have been proven to be particularly effective at detecting image activity along curves instead of radial directions [6]. We are currently investigating the use of curvelet-based texture descriptors and expect this to further improve the ability of our classifier to successfully classify each tissue sample.

To further validate the results obtained in this research,

the algorithm will be tested on a data set with supervised segmentation. The data set in this research project was segmented using and Active Contour Model algorithm; this was completed by non-radiologists. Application of this method to a radiologist-segmented data set might improve results. Since obtaining a radiologist segmented data set is not feasible, other segmentation algorithms for preprocessing steps are currently being investigated.

Organ	Texture	Sens.	Spec.	Prec.	Acc.
Backbone	Eng	88.4	96.0	82.3	94.7
	Ent	90.9	98.7	93.5	97.3
Heart	Eng	56.3	95.2	76.1	86.9
	Ent	77.8	97.9	90.8	93.6
Kidney	Eng	93.2	88.6	72.2	89.7
	Ent	94.2	92.3	79.4	92.7
Liver	Eng	68.6	94.9	76.8	89.7
	Ent	72.5	97.7	88.5	92.7
Spleen	Eng	62.5	92.9	65.0	87.6
	Ent	83.8	93.4	72.9	91.7
AVG	Eng	73.8	93.5	74.4	89.7
	Ent	83.8	96.0	85.0	93.6

Table 3: Feature analysis using L123

Organ	Texture	Sens.	Spec.	Prec.	Acc.
Backbone	L12	92.0	98.7	93.8	97.6
	L123	90.9	98.7	93.5	97.3
Heart	L12	78.0	97.0	87.4	92.9
	L123	77.8	97.9	90.8	93.6
Kidney	L12	94.8	94.0	83.2	94.2
	L123	94.2	92.3	79.4	92.7
Liver	L12	87.0	95.2	81.8	93.6
	L123	72.5	97.7	88.5	92.7
Spleen	L12	75.1	97.1	84.6	93.3
	L123	83.8	93.4	72.9	91.7
Average	1,2	85.4	96.4	86.2	94.3
	L123	83.8	96.0	85.0	93.6

Table 4: Resolution level analysis using Entropy features

Organ	Texture	Sens.	Spec.	Prec.	Acc.
Backbone	Wavelet	82.6	96.1	82.6	93.7
	Ridgelet	90.9	98.7	93.5	97.3
Heart	Wavelet	59.0	92.1	67.0	85.0
	Ridgelet	77.8	97.9	90.8	93.6
Kidney	Wavelet	77.7	91.4	69.9	88.6
	Ridgelet	94.2	92.3	79.4	92.7
Liver	Wavelet	87.3	94.4	82.6	92.8
	Ridgelet	72.5	97.7	88.5	92.7
Spleen	Wavelet	65.5	94.3	69.7	89.5
	Ridgelet	83.8	93.4	72.9	91.7
Average	Wavelet	74.4	93.7	74.4	89.9
	Ridgelet	83.8	96.0	85.0	93.6

Table 5: Comparison of the best ridgelet-based and wavelet-based description

References

[1] D. Xu, J. Lee, D.S. Raicu, J.D. Furst, D. Channin, Texture Classification of Normal Tissues in Computed Tomography. *The 2005 Annual Meeting of the Society for Computer Applications in Radiology*, Orlando, Florida, 2005.

[2] L. Semler, L. Dettori, J. Furst, Wavelet-Based Texture Classification of Tissues in Computed Tomography. *The 18th IEEE International Symposium on Computer-Based Medical Systems (CBMS'05)*, Dublin, Ireland, 2005, 265-270.

[3] M.N. Do, & M. Vetterli, The Finite Ridgelet Transform for Image Representation. *IEEE Transactions on Image Processing*, *12,* 2003, 16 – 28.

[4] H.E. LeBorgne, & N. O'Connor, Ridgelet-based Signatures for Natural Image Classification. *Advanced Concepts for Intelligent Vision Systems*, 2005, 20-23.

[5] E.J. Candes, & D.L. Donoho, Curvelets, Multi-resolution Representation, and Scaling Laws. *Wavelet Applications in Signal and Image Processing VIII, 4119-01*, 2000.

[6] J.L. Starck, D.L. Donoho, and E.J. Candes, Astronomical Image Representation by the Curvelet Transform. *Astronomy &Astrophysics, 398,* 1999, 785-800.

[7] B. Kara & N.Watsuji, Using Wavelets for Texture Classification. *Spelman Sci. & Math Journal, 1,* 1997, 22-31.

[8] A. Kurani, D.H. Xu, J.D. Furst, D.S. Raicu . Co-occurrence Matrices for Volumetric Data. *The 7th IASTED International Conference on Computer Graphics and Imaging*, Kauai, Hawaii, USA, 2004.

[9] D. H. Xu, A. Kurani, J. D. Furst, & D. S. Raicu, Run-length Encoding for Volumetric Texture. *The 4th IASTED International Conference on Visualization, Imaging, and Image Processing*, Marbella, Spain, 2004.